Journal of the European Ceramic Society **15** (1995) 145–153

0955-2219/95/$9.50

Surface Decontamination Treatments of Undoped $BaTiO_3$—Part II: Influence on Sintering

Claude Hérard, Annelise Faivre & Jacques Lemaître*

École Polytechnique Fédérale de Lausanne (EPFL), Laboratoire de Technologie des Poudres, MX-Ecublens, CH-1015 Lausanne, Switzerland

(Received 3 March 1994; revised version received 17 June 1994; accepted 30 June 1994)

Abstract

Natural sintering and microstructure of undoped $BaTiO_3$ ceramics obtained by slip casting from five commercial powders subjected to various surface decarbonation treatments (calcination and cleaning in pure water or acetate buffer solution) were investigated. Two densification steps followed in certain instances by a desintering step were observed for as-received powders. At maximum density the microstructure is either coarse-grained or bimodal, with dense large grains between 20 and 100 μm in a fine-grained matrix (<1 μm). At the end of swelling a coarse intergranular and fine intragranular porosity is present and total conversion into large grains has occurred, their size remaining unchanged up to 1400°C. Calcination and water cleaning had no noticeable influence on sintering behaviour. Acid cleaning appeared to substantially modify the shape of dilatometric curves: shrinkage starts later, the onset of abnormal grain growth is delayed, the maximum fired densities are slightly increased, but the subsequent swelling of specimens above 1300°C is also enhanced.

It is suggested that abnormal grain growth in undoped barium titanate results from the presence of a liquid phase at grain boundaries. Due to the presence of trace impurities, it can form locally at a temperature below the eutectic temperature of 1317°C of the system BaO–TiO_2. Decontamination by acid cleaning raises the eutectic point, but also increase the amount of liquid phase above 1300°C, by lowering the Ba content at the surface of the particles. The plasticity of the material is then increased, promoting swelling due to internal CO_2 pressure, originating from the decomposition of $BaCO_3$ which still subsists after acid cleaning.

* To whom correspondence should be addressed.

1 Introduction

Electrical properties of structural ceramics are strongly dependent on their microstructure. This is particularly true in the case of $BaTiO_3$-based capacitors, where exaggerated final porosity drastically decreases the dielectric strength and the dielectric constant.[1] The porosity evolution during sintering is often complicated by the presence of impurities and by anomalous grain growth.[2] The possibility of obtaining fully dense sintered materials is then greatly related to the impurity content in initial powders.

This is the second part of a series of two papers dealing with surface contamination effects in undoped barium titanate. It was shown in Part I[3] by chemical analyses that an important source of contamination for $BaTiO_3$ raw powders is barium carbonate, resulting from reaction of the surface with atmospheric CO_2 or formed during the synthesis of the powders, which is distributed mainly at the surface of the particles and which thermally decomposes in two steps near 700 and 1300°C to release CO_2; thermal (calcination) or chemical (cleaning in a pH 4·5 acetate buffer) treatments of different undoped barium titanate commercial powders proved to be an efficient way to reduce the surface $BaCO_3$ content. The effects of such treatments on forming green bodies by slip casting were described, the corresponding improvement in green density being ascribed to the reduction of agglomerates in the starting slips. The work presented in the present paper is focused on the sintering stage of such thermally and chemically surface decarbonated $BaTiO_3$ powders. Sintering kinetics in air were monitored by dilatometry and optical microscopy on slip-cast green bodies obtained from five commercial powders, subjected to the decontamination treatments reported in Part I.[3] Densification and grain growth processes are discussed and interpreted in terms of internal gas

release and the presence of a liquid phase correlated with the surface chemical composition of the powders.

2 Experimental Procedure

The five commercial $BaTiO_3$ powders used in this study, Criceram lot VPP20, TAM HPB lot 688, TAM HPB lot 745, Cabot BT10 lot 6243-24, and Rhône-Poulenc type Elmic BT 100 lot 7958, are described in Part I,[3] along with the de-agglomeration and decontamination treatments performed (calcination at 500°C for 16 h, acid cleaning in a 0·3M acetate buffer with pH = 4·5 for 16 h at 30°C, and demineralised water cleaning).

For each powder source and each treatment *slip-cast specimens* were prepared from aqueous $BaTiO_3$ suspensions stabilised with poly(acrylic acid)(PAA), with [PAA] ranging from 0·6 to 1 wt%. The acidity of the stabiliser was neutralised by NH_3, with $[NH_3]/[PAA] = 1·5$. The amount of dispersing liquid was between 135 and 270 μlitre/g. The methodology used is described in Part I.[3]

Non-isothermal *sintering* of the compacts was studied in dry air in a differential dilatometer Setaram DHT; the heating cycle was 10°C/min up to 800°C, 3·3°C/min up to 1400°C, and 5°C/min down to 20°C.

Fired densities were measured by Archimedes' method, using isopropanol as immersion liquid, and assuming the value of 6·02 g/cm^3 for the theoretical density of $BaTiO_3$. Intermediate fired densities were either calculated from dilatometric curves corrected for thermal expansion and calibrated with respect to measured final densities (i.e. at the end of the thermal cycle), or measured directly on specimens whose heating cycle was interrupted at some particular temperature.

Microstructures were observed with a Olympus type BHM optical microscope on polished and thermally etched samples (heating rate: 5°C/min from 20 to 1200°C then down to 20°C in air).

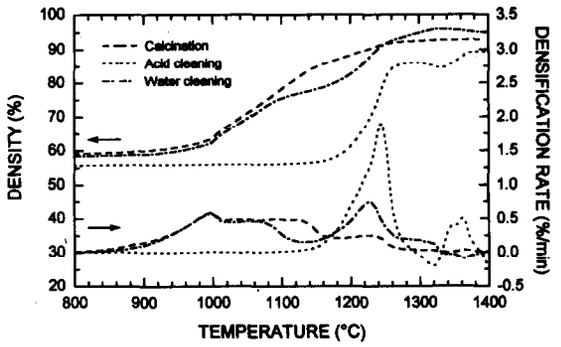

Fig. 2. Dilatometric curves for Cabot powder.

3 Results

3.1 Dilatometry

The sintering behaviour of raw powders is illustrated by dilatometric curves shown in Fig. 1. Criceram, TAM 688 and TAM 745 raw powder curves present a similar shape: shrinkage starts at 1050°C and two distinct densification peaks appear between 1240 and 1340°C. The density passes through a maximum beyond which swelling of the samples occurs, followed by a small redensification step.

The Rhône-Poulenc raw powder exhibits a quite different behaviour: shrinkage starts earlier (800°C) due to the smaller mean particle size, densification progresses continuously up to 1400°C and is not completed at this temperature. (Cabot raw powder could not be sintered because cast green bodies were too brittle).

Dilatometric curves of calcined, acid-cleaned and water-cleaned powders can be seen in Figs 2–6 along with raw powder curves for comparison. The same trend is again found for Criceram, TAM 688 and TAM 745 powders: the general shape of the densification curves is not modified, although acid cleaning slightly increases the maximum density, the corresponding temperature being slightly increased. However, the subsequent desintering step is amplified (up to 8% theoretical density for TAM 745 2nd Criceram powders) and its corresponding temperature increased. Water cleaning has no effect on calcined powders, and calcination alone only reduces the shrinkage

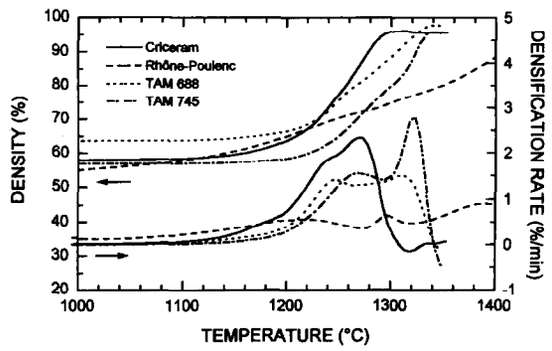

Fig. 1. Dilatometric curves for raw powders.

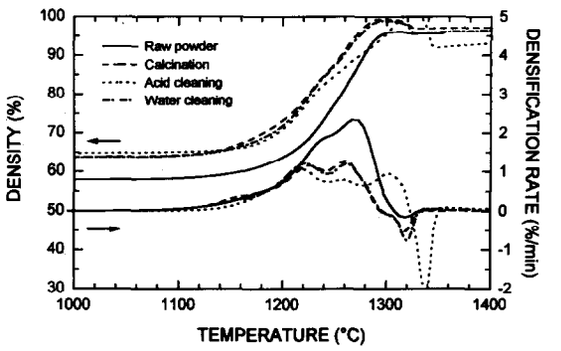

Fig. 3. Dilatometric curves for Criceram powder.

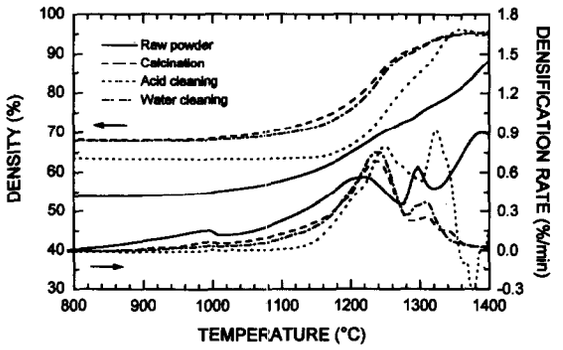

Fig. 4. Dilatometric curves for Rhône-Poulenc powder.

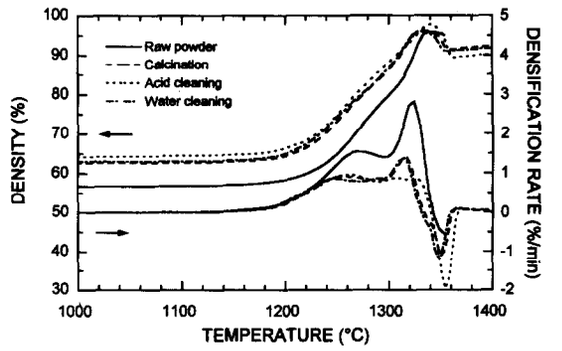

Fig. 6. Dilatometric curves for TAM 745 powder.

(because of a higher green density) to finally yield the same maximum density as raw powders. Treatments on the Rhône-Poulenc powder have drastically changed the sintering kinetics. Densification of the calcined powder is almost complete at 1400°C, maximum density has been increased and the beginning of densification is slightly delayed. Water cleaning does not affect the calcined powder, and the densification of acid cleaned powder starts later near 1100°C and then presents two peaks followed by a desintering step, as for Criceram and TAM powders. The sintering of calcined and water-cleaned Cabot powders starts at 800°C, and is continuous up to 1330°C. After acid cleaning it starts at 1100°C and a sharp densification rate peak is seen at 1240°C followed by a weak dedensification and then redensification step providing a lower density than calcined or water-cleaned powders. Figure 7 shows the maximum fired densities for all powders and treatments, which are not correlated with green densities and range between 95 and 100% except for Cabot powder. Calcination and water cleaning have no significant effect on maximum fired density, but acid cleaning slightly increases it, except for Criceram and Rhône-Poulenc powders.

3.2 Microstructures

In order to understand the mechanisms involved in the densification process the heating cycles of some specimens were interrupted at the temperature of maximum density and at the end of swelling in order to observe the corresponding microstructures. For all powders calcination and water cleaning have no noticeable effect on microstructure compared to raw powders.

At *maximum density* between 1300 and 1400°C the microstructure is bimodal for TAM 745, TAM 688 and Criceram raw powders (dense large grains of about 50–70 μm in a fine-grained matrix), while for Rhône-Poulenc raw powder it is entirely formed of large grains of about 100 μm with fine intragranular porosity. Acid cleaning decreases the proportion of large grains for the TAM and Criceram powders, and renders bimodal the microstructure of Rhône-Poulenc powder, which is now similar to that of TAM and Criceram powders. Calcined and water-cleaned Cabot powder microstructure at maximum density is formed of large grains (100 μm). Their size is reduced to 50 μm by acid cleaning, accompanied by the development of coarse inter- and intragranular porosity.

For powders presenting a dedensification step beyond the maximum density (TAM 745, TAM 688, Criceram, water and acid-cleaned Cabot and acid-cleaned Rhône-Poulenc powders) total conversion into large grains has occurred at the secondary *relative minimum density*, which is the point where the samples begin to redensify. At this point, an important porosity can be seen, both intra- and intergranular, the latter resulting from pore coalescence, and increased by acid cleaning. As the temperature goes up, some specimens slightly redensify, (TAM 745, Criceram) but grain size remains unchanged. This behaviour is

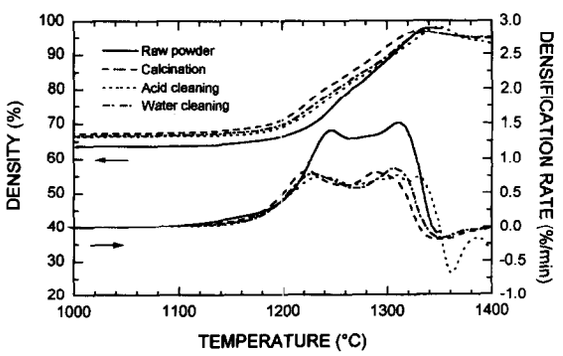

Fig. 5. Dilatometric curves for TAM 688 powder.

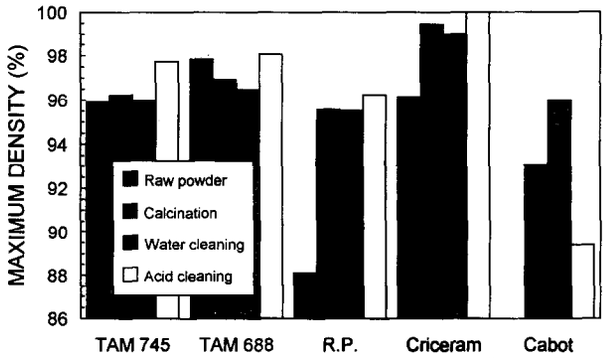

Fig. 7. Effects of treatments on maximum fired density.

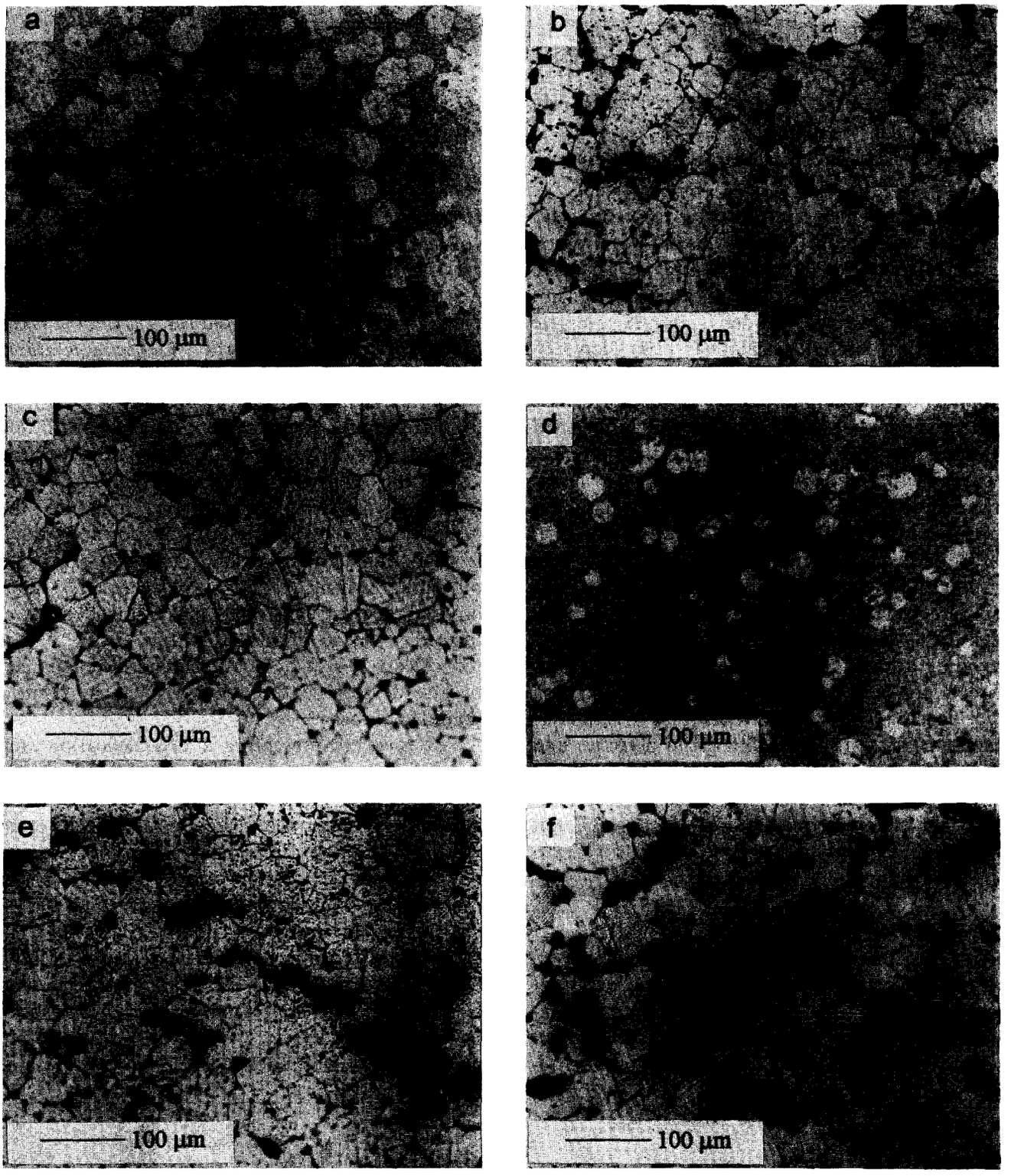

Fig. 8. Microstructure of Criceram samples: (a) Calcined powder at maximum density (1295°C); (b) calcined powder at the end of swelling (1338°C); (c) calcined power at 1400°C; (d) acid cleaned at maximum density (1324°C); (e) acid cleaned at the end of swelling (1352°C); (f) acid cleaned at 1400°C.

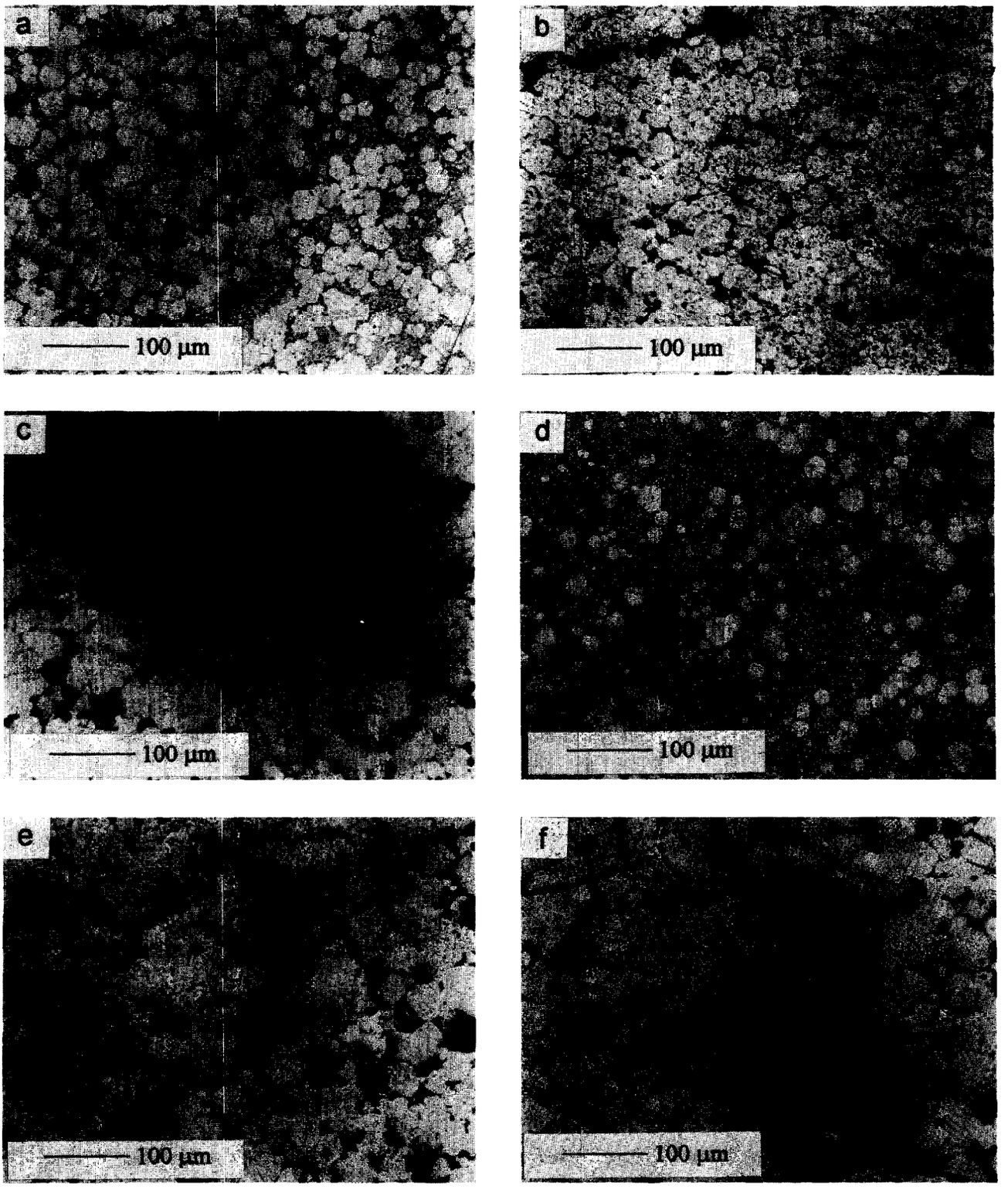

Fig. 9. Microstructure of TAM 745 samples: (a) Calcined powder at maximum density (1334°C); (b) calcined powder at the end of swelling (1363°C); (c) calcined powder at 1400°C; (d) acid cleaned at maximum density (1341°C); (e) acid cleaned at the end of swelling (1367°C); (f) acid cleaned at 1400°C.

Table 1. Density evolution during sintering.

Powder	*Treatment*	*Green density (%)*	*Maximum density (%)*	*Temperature for maximum density (°C)*	*Density after swelling (%)*	*Temperature at the end of swelling (°C)*
TAM 745	Raw	59·0	95·9	1338	—	—
	Calcined	64·0	96·2	1334	91·6	1363
	Acid cleaning	64·6	97·7	1341	89·6	1367
	Water cleaning	65·1	96·0	1331	91·1	1360
TAM 688	Raw	66·7	97·8	1342	—	—
	Calcined	69·0	96·9	1330	94·5	1400
	Acid cleaning	68·5	98·1	1351	92·7	1400
	Water cleaning	68·8	96·5	1337	94·7	1400
Criceram	Raw	58·8	96·1	1315	95·7	1334
	Calcined	63·4	99·4	1295	97·0	1338
	Acid cleaning	63·6	100·0	1324	92·1	1352
	Water cleaning	63·4	99·0	1297	95·7	1334
Rhône-Poulenc	Raw	57·1	88·1	1400	—	—
	Calcined	66·9	95·6	1400	—	—
	Acid cleaning	66·5	96·3	1355	94·8	1395
	Water cleaning	66·5	95·5	1400	—	—
Cabot	Raw	—	—	—	—	—
	Calcined	57·1	93·1	1400	—	—
	Acid cleaning	57·6	89·4	1385	84·6	1332
	Water cleaning	58·8	96·0	1328	95·1	1396

exemplified by microstructures of calcined and acid-cleaned Criceram and TAM 745 powders shown in Figs 8 and 9. The case of acid-cleaned Cabot powder is particularly interesting because it presents two consecutive desintering steps, near 1290 and then 1385°C. At the end of the heating cycle (1400°C) the microstructures are coarse-grained for all powders and treatments, with an important porosity, increased by acid cleaning. This treatment does not affect the final grain size for TAM 688, TAM 745 and Criceram powder (40 μm), but decreases it for Cabot and Rhône-Poulenc powders, from 100 to 40 μm (cf. Fig. 10).

Measured densities of specimens at the beginning of sintering, at maximum density and at the end of swelling when present are reported in Table 1, along with corresponding temperatures, for all powders and treatments.

4 Discussion

4.1 Raw powders

The apparent decrease in densification rates of treated powders compared to untreated ones is a mere consequence of the improvement of the green densities. It provides also slight but significant enhancements in the maximum fired density, except for Cabot powder, as shown in Table 1. The difference between sintering behaviour of raw powders is probably due to their particle size and specific surface contamination, resulting from both their history and their synthesis route.

Sintering of the larger particle raw powders (TAM 688, TAM 745, Criceram—d_{v50} about 1·4 μm) looks similar: during the initial stage, up to 1100°C, the compacts consolidate without densification. The first densification peak, corresponding

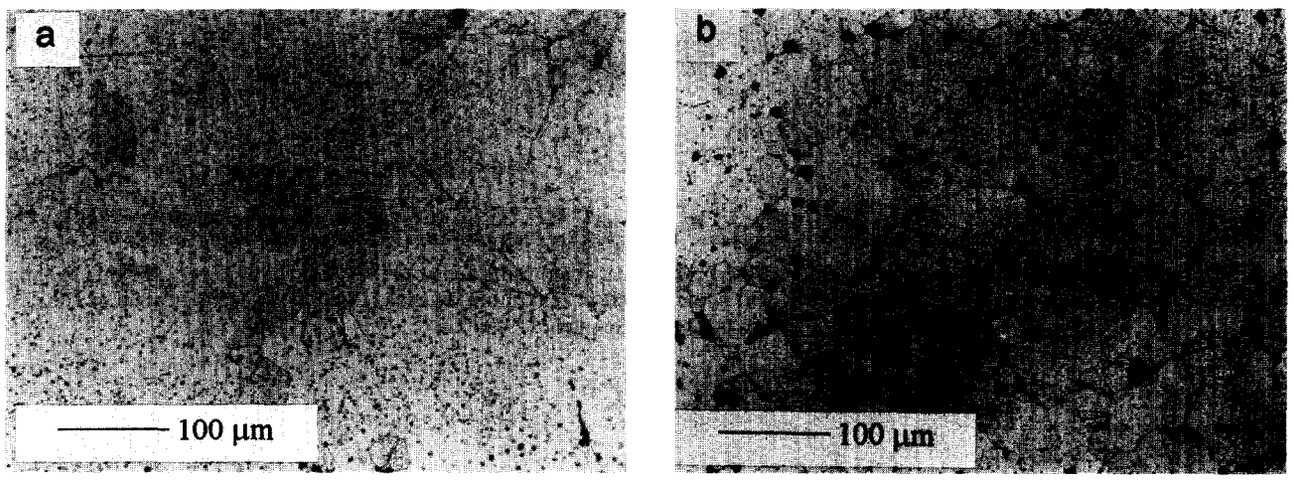

Fig. 10. Microstructure of Rhône-Poulenc samples at 1400°C: (a) Water-cleaned powder, (b) acid-cleaned powder.

to the intermediate stage, may be ascribed to normal grain growth, which progresses by bulk and boundary diffusion[4] as long as diffusion paths are not too long. At this point the most favourable mechanism to reduce surface free energy is abnormal grain growth, i.e. growth of large grains at the expense of smaller ones, which corresponds to the final stage and can account for the second densification peak. Abnormal grain growth, by reduction of the boundary areas, leads to pore coalescence. However, if this stage is too fast some pores may remain trapped inside large grains, lowering the maximum density. The temperature at which abnormal grain growth starts is correlated with the impurity content, as will be discussed later. Once total conversion into large grains has occurred, a desintering step is observed (cf. Figs 3, 5 and 6). A fine intragranular porosity is then present at the secondary minimum density which was absent at maximum density (Figs 8(a), 8(d), 9(a) and 9(d)), suggesting internal gas release. When the temperature increases, fine intragranular pores condense at the boundaries, giving rise to temporary interconnected open porosity (Figs 8(b), 8(e), 9(b) and 9(e)); at this stage evolved gas can escape from the body and further densification can occur. At 1400°C intragranular porosity has disappeared, leaving mainly intergranular porosity (Figs 8(c), 8(f), 9(c) and 9(f)).

A smaller powder such as Rhône-Poulenc (d_{v50} = 0·84 μm) is more reactive; as a result it densifies earlier, as soon as 800°C is reached (see Fig. 4). This fast shrinkage prevents the efficient removal of porosity (pore trapping), eventually yielding a low density at 1400°C. The final coarse-grained microstructure presents an homogeneously distributed intragranular porosity, which has not yet condensed at the boundaries.

4.2 Gas release

It was shown in Part I[3] by TGA and FT-IR that only CO_2 was released up to 1400°C, besides water evolution below 200°C; therefore it is suggested that CO_2 released from barium carbonate decomposition is responsible for the swelling phenomenon, because of its low solubility in $BaTiO_3$. CO_2 release in the 500–900°C range has been shown to be due to $BaCO_3$ reaction with TiO_2 to form $BaTiO_3$ (reaction (1) in Part I[3]), which does not interact with densification because porosity is still open at that temperature, so that CO_2 can escape from the compact material. The second $BaCO_3$ decomposition step near 1300°C, by reaction with $BaTiO_3$ to form Ba_2TiO_4 and CO_2 (reaction (2) in Part I[3]), undoubtedly promotes swelling at that temperature, because the porosity is then closed. The CO_2 decomposition pressure P_d for reaction (2) of Part I_3 was calculated using:

$$P_d = \exp\left(-\frac{(\Delta H^\circ - T\Delta S^\circ)}{RT}\right) \quad (1)$$

where ΔH° and ΔS° are respectively the standard enthalpy and entropy of reaction (2) of Part I[3] R the gas constant and T the absolute temperature. Thermodynamic data give ΔH° = 178 kJ/mol and ΔS°= 140·3 J/mol K at 1300°C,[5] so P_d is about 2·8 MPa; such a pressure is larger than the stress necessary to initiate plastic deformation of fine-grained $BaTiO_3$, which is 2MPa at this temperature,[6] allowing swelling and the observed bloating phenomenon. Table 2 shows measured weight losses between 1100 and 1400°C and the corresponding gas volume produced at 2 MPa and 1400°C. Based upon the lowest of these figures (0·007% weight loss between 1200 and 1400°C for TAM 745 powder) and using perfect gas law, a density decrease down to 6·2% below the maximum value can then be explained, which is consistent with the desintering magnitudes observed.

4.3 Effects of the treatments

As already mentioned, calcination and water cleaning have no noticeable effect on the sintering of TAM 688, TAM 745 and Criceram powders, while they improve the final density of Rhône-Poulenc powder, which shows the same coarse-grained porous microstructure as the untreated powder. Calcined and water-cleaned Cabot powders densify approximately the same way, which is different from the other powders. On the other hand, the sintering behaviour of all powders is substantially modified by acid cleaning, giving rise to more similar dilatograms and final microstructures. The most remarkable effect of acid cleaning is the moving from 800°C up to 1100°C of the incipient sintering temperature for the Rhône-Poulenc and Cabot powders. As mentioned before the technical data sheets indicate approximately the same level for various impurities in all powders. However, due to their smaller particle sizes, the Cabot (0·4 μm) and Rhône-Poulenc (0·84 μm) samples are likely to be decontaminated more

Table 2. Weight losses between 1100 and 1400°C (measured by TGA) and corresponding CO_2 volume produced at 2 MPa and 1300°C

Powder	*CO_2 (wt%) released between 1100 and 1400°C*	*Gas volume (%) at 2 MPa–1400°C*
TAM 745	0·007	6·2
TAM 688	0·022	17·3
Criceram	0·017	13·9
Rhône-Pulenc	0·116	52·5
Cabot	0·087	45·3

thoroughly upon acid leaching; as a consequence, one may expect that acid washing will suppress any sintering phenomena below 1100°C but surface diffusion, therefore suppressing any shrinkage below that temperature.

The delay of the onset of abnormal grain growth by acid cleaning can be explained under the assumption that this last phenomenon is triggered by the formation of a liquid phase at the boundaries, even in raw powders. Examination of Fig. 1 shows that the onset temperature of the second densification peak corresponding to abnormal grain growth may be located, for some raw powders and in particular Criceram, below the eutectic temperature of 1317°C in the BaO–TiO_2 diagram.[7] However, impurities such as Si, Al or Na are generally present in commercial undoped barium titanate: between 20 and 100 ppm according to the suppliers of the powders used in this study. Ternary diagrams of such compositions show that the eutectic point can be drastically lowered, down to 1250°C, for example, for the system $BaTiO_3$–SiO_2 or even 942°C for the system $NaSiO_3$–$BaTiO_3$.[8] Compositional fluctuation of impurities can then give rise locally to sufficiently concentrated zones to form a liquid phase at the boundaries and consequently constitute nuclei for exaggerated grain growth by a dissolution–precipitation mechanism (Ostwald ripening)[9] at temperatures far below 1317°C. Abnormal grain growth has already been reported in $BaTiO_3$ below 1322°C in the absence of a liquid phase,[10] with twinned platelike grains growing by a solid-state process. In contrast, the rounded shape of large grains found below 1317°C in the present samples strongly indicates the presence of a liquid phase. Acid cleaning, by removing such melting agent impurities from the surface of the particles, raises the eutectic point to the expected value near 1320°C for 'pure' $BaTiO_3$ and consequently retards and slows down abnormal grain growth. Dilatometric curves for TAM 688 powder (Fig. 5) reveal only a weak contamination, the position of the second densification peak and maximum density being only slightly shifted (about 10°C). Conversely, Criceram powder appears to be more contaminated (Fig. 3): the second densification peak occurs at 1270°C for raw powder and is shifted to 1301°C after acid cleaning.

Despite the fact that surface barium carbonate is greatly reduced after acid cleaning, this treatment promotes an unexpected enhancement of the desintering stage on TAM 688, TAM 745 and Criceram powders. Rhône-Poulenc and Cabot powders present a desintering stage after acid cleaning only. The same phenomenon was observed on annealing hot-pressed samples (TAM 688), compacts being obtained without organic additive (PAA): therefore it is concluded that PAA decomposition plays no role in swelling, which is only due to $BaCO_3$ decomposition. XPS, EGA and TGA investigations[3] show that barium carbonate is still found after acid cleaning; the thermogravimetric weight losses between 1200 and 1400°C after acid cleaning are the same as for the raw powders, indicating that the acid-cleaning solution used was not strong enough to dissolve the $BaCO_3$ completely. Discrete $BaCO_3$ particles are not likely to be present after acid cleaning, unless they are trapped inside $BaTiO_3$ grains. It is more probable that a layer of carbonate more strongly bonded to the surface subsists, as shown by XPS, this remaining quantity corresponding to the weight losses shown in Table 2. These weight losses, if assumed to produce CO_2, are sufficient to account for desintering amplitudes as high as those observed for TAM 745 and Criceram acid-cleaned powders (8%). The magnitude of swelling is not proportional to the residual barium carbonate content—provided it is greater than 0·03 wt%—because once the porosity opens again, CO_2 can escape freely from the material.

The *increase* in swelling after acid cleaning results from a secondary effect of this treatment. During acid cleaning some Ba^{2+} ions were dissolved from the surface of the particles, which consequently become barium deficient, as shown by XPS in Part I.[3] This means that the isocompositional line has been shifted towards the TiO_2 side: the amount of liquid phase present at grain boundaries above 1300°C is then increased. As a consequence the plasticity of the material is enhanced, hence promoting swelling upon the development of internal CO_2 pressure inside the samples.

5 Conclusions

The effect of decontamination treatments of the surface of $BaTiO_3$ powders on sintering was investigated. Calcination only improves green densities of slip-cast bodies, which then densify upon sintering in more or less the same way as raw powders. Acid cleaning has extra repercussions on the sintering stage: increases in green densities combined with a delayed abnormal grain growth improve the elimination of porosity during the first stage of sintering, yielding slightly higher maximum densities. However, swelling above 1300°C is also increased, resulting from the development of internal CO_2 pressure inside the samples at high temperature after closure of the porosity. This carbon dioxide release originates from the decomposition of residual $BaCO_3$ which still subsists after acid cleaning. It is argued that impurities com-

monly found in undoped $BaTiO_3$ can promote the formation of a liquid phase at lower temperatures, responsible for abnormal grain growth. The formation of this liquid phase, and consequently the microstructure, can be controlled by acid cleaning, by eliminating both the melting agents present as impurities, and changing the surface Ba/Ti ratio. Complete removal of surface $BaCO_3$, using more acidic cleaning solutions, could lead to fully dense specimens by suppressing gas release at high temperature, assuming no $BaCO_3$ in the bulk.

Processing of commercial $BaTiO_3$ raw powders, especially by acid cleaning, appears to be beneficial on final properties. Removal of most of the barium carbonate by this treatment and various impurities hardly quantifiable present at the surface of the particles give rise to an approximately similar sintering behaviour for all powders. A similar final microstructure less sensitive to the starting commercial powder can then be obtained, confirming the great influence of the surface chemistry of initial powders on the final properties of the ceramics made thereof.

Acknowledgements

The Swiss National Foundation is gratefully acknowledged for financial support. The authors would like to thank Dr P. Bowen for his assistance in the preparation of the manuscript and Prof C. Carry for fruitful discussions.

References

1. Gerson, R. & Marshall, T. C., Dielectric breakdown of porous ceramics. *J. Appl. Phys.*, **30**(11) (1959) 1650–3.
2. Xue, L. A. & Brook, R. J., Promotion of densification by grain growth. *J. Am. Ceram. Soc.*, **72**(2) (1989) 341–4.
3. Hérard, C., Faivre, A. & Lemaître, J., Surface decontamination treatments in undoped $BaTiO_3$. Part I: Powder and green body properties. *J. Eur. Ceram. Soc.*, (1994) (1442).
4. Kingery, W. D., Bowen, H. K. & Uhlmann, D. R., *Introduction to Ceramics*. John Wiley and Sons, NY, 1976.
5. Barin, I. & Knacke, O., *Thermochemical Properties of Inorganic Substances*. Springer, Berlin, 1973.
6. Carry, C. & Mocellin, A., Superplastic creep of fine grained $BaTiO_3$ in a reducing environment. *J. Am. Ceram. Soc.*, **69**(9) (1986) C215–16.
7. Rase, D. E. & Roy, R., Phase equilibria in the system BaO–TiO_2. *J. Am. Ceram. Soc.*, **38**(3) (1955) 102–13.
8. Levin, E. M., Robbins, C. R. & McMurdie, H. F., *Phase Diagrams for Ceramists*. American Ceramic Society, Colombus, 1964.
9. Hennings, D. F. K., Janssen, R. & Reynen, P. J. L., Control of liquid phase-enhanced discontinuous grain growth in barium titanate. *J. Am. Ceram. Soc.*, **70**(1) (1987) 23–7.
10. Schmelz, H. & Meyer, A., The evidence of anomalous grain growth below the eutectic temperature in $BaTiO_3$ ceramics. *Ber. Dtsch. Keram. Ges.*, **59**(8/9) (1982) 436–40.